Atmos. Meas. Tech. Discuss., https://doi.org/10.5194/amt-2018-394
Manuscript under review for journal Atmos. Meas. Tech.
Discussion started: 4 December 2018

Atmospheric Measurement Techniques Discussions

A portable dual smog chamber system for atmospheric aerosol field studies

Christos Kaltsonoudis[1,2,3], Spiro D. Jorga[3], Evangelos Louvaris[1,2], Kalliopi Florou[1,2] and Spyros N. Pandis[1,2,3]

[1]Institute of Chemical Engineering Sciences, ICE-HT, Patras, Greece
[2]Department of Chemical Engineering, University of Patras, Patras, Greece
[3]Department of Chemical Engineering, Carnegie Mellon University, Pittsburgh, USA

Abstract

Smog chamber experiments using as a starting point ambient air can improve our understanding of the evolution of atmospheric particulate matter at timescales longer than those achieved by traditional laboratory experiments. These types of studies can take place under more realistic environmental conditions addressing the interactions among multiple pollutants. The use of two identical smog chambers, with the first serving as the baseline chamber and the second as the perturbation chamber (in which addition or removal of pollutants, addition of oxidants, change in the relative humidity, etc.), can facilitate the interpretation of the results in such inherently complex experiments. The differences of the measurements in the two chambers can be used as the basis for the analysis of the corresponding chemical or physical processes of ambient air.

A portable dual smog chamber system was developed using two identical pillow-shaped smog chambers (1.5 m^3 each). The two chambers are surrounded by UV lamps in a hexagonal arrangement yielding a total J_{NO2} of 0.1 min^{-1}. The system can be easily disassembled and transported enabling the study of various atmospheric environments. Moreover, it can be used with natural sunlight. The results of test experiments using ambient air as starting point are discussed as examples of applications of this system.

1. Introduction

Teflon reactors, known as smog or atmospheric simulation chambers have been valuable research tools for the study of the complex chemical interactions that take place in the atmosphere. Studies using such reactors date back to the 1950s (Finlayson and Pitts, 1976). The use of these chambers eliminates many of the uncertainties resulting from the analysis of ambient observations where

several variables, such as weather conditions, pollutant emission rates, dilution and transport are all contributing to the observed changes (Kim et al., 2009). Typically, these reactors are made of Teflon, though there are some chambers that are made of metal or glass (Cocker et al., 2001a; Paulsen et al., 2005; Kim et al., 2009). The volume of these chambers varies from a few hundred liters up to hundreds of cubic meters, with the larger configurations having lower surface to volume ratio, thus minimizing the wall effects (Cocker et al., 2001a).

Chambers are placed either indoors or outdoors with the former having the advantage of a well-controlled environment with constant temperature, light intensity etc. and the latter being able to use natural sunlight (Laity, 1971; Jeffries et al., 1976; Leone et al., 1985; Carter et al., 2005). For the indoor chambers, a variety of UV light sources can be used including black light lamps (Laity, 1971), xenon, and argon arc lamps (Warren et al., 2008). Some chamber facilities include two identical smog chambers in order to use the first chamber as a reference (Kim et al., 2009). This practice can enhance the quality of the results since numerous variables can have an effect on the outcome of each experiment.

Different groups around the world have conducted thousands of smog chamber experiments in order to simulate the behavior of pollutants in ambient air. These smog chambers have been used to study, for example, secondary organic aerosol and its dependence on temperature, relative humidity, UV intensity, NO_x levels, etc. (Halquist et al., 2009; Tritscher et al., 2011). Other studies have focused on the characterization and evolution of primary emissions from selected sources (Weitkamp et al., 2007; Kostenidou et al., 2013; Platt et al., 2013).

There have been a number of studies that used ambient air as the starting point of the experiment. Roberts and Friedlander (1976) added SO_2, 1-heptene and NO_x to a 96 m^3 outdoor chamber filled with ambient air to study the aerosol formation. Heisler et al. (1977) used ambient air to fill an outdoor 80 m^3 Teflon chamber to study the growth rate of the particles. Pitt et al. (1977) concluded that the addition of N,N'-diethylhydroxylamine in ambient air enhances the formation of ozone, peroxyacetyl nitrate, and light-scattering particles. Kelly (1987) used a 0.5 m^3 chamber to investigate the HNO_3 formation in ambient air. Kelly and Gunst (1990) studied the ozone dependence on hydrocarbons and nitrogen oxide using ambient air. Lee et al. (2010) investigated the correlations between light intensity and ozone formation for ambient air in Seoul. The potential OA enhancement or sink due to aging of ambient air has been also studied in the field by the use of oxidation flow reactors (OFR) in various ambient environments (Tkacik et al.,

2014; Ortega et al., 2016). The OFR uses high OH levels, thus simulating atmospheric oxidation in timescales of several days to weeks. On the other hand, typical experiments in atmospheric simulation chambers take place at close to ambient OH levels and simulate hours to a few days of aging.

There have been a few efforts to use portable smog chamber facilities for different applications. For example, Shibuya et al. (1981) used a portable 4.5 m^3 smog chamber, installed in a vehicle, to study the ozone formation in ambient air. Hennigan et al. (2011) and Stockwell et al. (2014) developed portable twin-chamber systems with UV lights to monitor the aging of combustion emissions. A portable smog chamber facility was also developed by Platt et al. (2013) featuring a 9 m^3 Teflon reactor that can be mounted on a trailer.

Typically, smog chamber experiments isolate a pollutant or a mixture of pollutants emitted by a source and focus on its chemistry. In most cases, clean air is used as the starting point of the experiment. While the corresponding results are clearly valuable, these experiments might miss the potentially important interactions of the examined chemical system with other pollutants existing in ambient air. To close this major gap between the laboratory studies and the ambient atmosphere, a portable dual smog chamber system with UV lights is designed and tested in this study. The chamber has been developed to use ambient air rather than clean air as its starting point. Having the advantage of being portable enhances the opportunities to study several environmental scenarios and simulate the processes occurring in previously out-of-reach chemical regimes (e.g., very aged air masses). The preliminary tests of the operation of this system are presented.

2. Design of the dual smog chamber system

2.1 Smog chambers

Relatively small Teflon reactors were selected for this system so that they can be filled in a matter of minutes, while having a volume adequate to support a 4-hour batch experiment, losing less than a third of their volume based on the standard instrumentation sampling flow rates. A set of two identical smog chambers was constructed from Teflon (PTFE) 0.2 μm film. Each chamber has a nominal volume of 1.5 m^3. The two chambers are pillow-shaped and are permanently mounted on a metal frames (Figure 1a). The relatively small volume of the chambers along with the fixed frame enables their easy and safe transport without having to disassemble them or to remove the sampling ports. Relative humidity (RH) and temperature sensors are also fixed on the chambers. The frame

dimensions are 1.7 x 0.5 x 1.7 m. Two sampling ports (one per chamber) with multiple lines and a temperature / RH sensor were installed on the reactors.

Sampling is alternated between the two chambers every three minutes by an automated three-way valve synchronized with the operation of the corresponding instrumentation. This allows a total duration of the experiments of more than 4 hours without the addition of make-up air. In order to eliminate interferences and memory effects due to this periodical alteration of the sampling lines, adequate time (30 s) is allowed within the three-minute sampling cycle for the lines to be flushed with the sample air from the next chamber. This is achieved by synchronizing the line flushing with the measuring instrumentation and discarding the data collected during this 30 s period.

2.2 Portable UV lighting system

A hemispheric design was selected with sixty 36 W UV light lamps (Osram, L36W/73) in a hexagonal arrangement. The lamps were mounted on five metal frames (12 per frame) creating five sub-structures (Figure 1b) that can be easily disassembled and transported. Once assembled the UV light support structure had a footprint of 4.5 x 4.5 m and a height of 2.5 m. Figure 1b shows the UV light assembly without the covering material. Flexible tent poles were used to create a dome that can be partially or fully covered protecting the chambers from the elements (Figures 1c and 1d). The sixth side does not include lights and is used as an entrance for chamber maintenance. The lights can be remotely operated at 20, 40, 60, 80 and 100% levels. The light fixtures include aluminum mirrors in order to direct the light towards the center of the dome, thus maximizing the light intensity delivered to the chambers. When all lights are on, the corresponding J_{NO2} is 0.1 min^{-1}. The two chambers are placed inside this dome having at least a 0.5 m clearance from the UV lights when full. This design also allows the use of a single 10 m^3 chamber if so desired.

2.3 Subsystems

A dual-head metal bellows pump (model MB-602) is used to fill the chambers with ambient air delivering 80 L min^{-1} per pump head. Both chambers can be filled in around 20 minutes. Manual two-way valves were installed prior to the chamber inlets for isolation and selective filling purposes. Prior to any experiment with ambient air, both chambers are flushed with ambient air with the metal bellows pump until the NO_x and O_3 levels matched the ambient concentrations. To

ensure chamber similarity the chambers are used alternatively in experiments as a perturbation/reference chamber.

If required clean particle free air can be introduced in the chambers. Dry air is generated by an oil-less compressor (Bambi VT200D) and further purified by activated carbon (Carbon cap, Whatman), HEPA filters (HEPA capsule, Pall) and silica gel (Silica gel rubin, Sigma-Aldrich). A subunit including the above systems (except for the filling pump and the compressor) was added to one of the metal frames of the system. This subunit also includes a syringe pump, an atomizer (TSI model 3076) and a silica gel diffusion drier (Silica gel rubin, Sigma-Aldrich) for seed generation. Additionally, a bubbler subsystem for HONO introduction and an ozone generator (Azcozon, model HTU-500) were used. Two temperature/RH sensors (Omega, model RH-usb) and a personal computer with Labview control for the sampling selection valve are also part of this system.

2.4 Instrumentation

The set of instruments selected for the use with the chamber system include: a HR-ToF-AMS (Aerodyne Research Inc.), a PTR-MS (Ionicon Analytik), a Scanning Mobility Particle Sizer (SMPS, classifier model 3080, DMA model 3081, CPC model 3787, TSI), an ozone monitor (API Teledyne, model 400E) and a NO_x monitor (API Teledyne, model T201). These instruments are located inside the FORTH mobile laboratory (Fig 1c) next to the chambers. Details on the instrumentation used can be found elsewhere (Kostenidou et al., 2013; Kaltsonoudis et al., 2016, Florou et al., 2018). With this configuration, a total sampling flow rate of 2.5-3 L min^{-1} is used that removes less than 0.1 m^3 from each chamber per hour.

2.5 Experimental procedure

The instrumentation is first used to characterize the ambient conditions for at least a couple of hours. After filling of the chambers is completed, sampling is switched from ambient measurements to the chambers and an initial characterization of the sampled air inside the chambers takes place. Then a perturbation (addition of oxidant or pollutant) is implemented in one of the chambers, while the other is used as a reference. Following the completion of the experiment ammonium sulfate seeds are introduced into both chambers to measure their loss rate on the walls over time. In this step, the chambers may be refilled with particle free air. This last stage is used

to quantify the particle size-dependent wall loss rate constants in order to make corrections to the rest of the measurements. Finally, the instrumentation is switched back to ambient observations and the chambers are flushed with either ambient air and /or clean air in preparation for the next experiment.

3. System evaluation

The system was developed and evaluated in Patras, Greece and also during the Finokalia Aerosol Measurement Experiment (FAME 16) campaign. Finokalia is a remote site in Crete, Greece (Kouvarakis et al., 2000). The field campaign took place during May-June 2016. Additional tests aimed on improving the performance of the setup were performed indoors at Carnegie Mellon University in Pittsburgh, United States.

3.1 Contamination tests

Tests were conducted in the field in order to assess the potential contamination of the chambers by ambient air. The chambers were filled with clean (particle free) air and the particle concentration inside the chambers was monitored by an SMPS. Figure 2 shows the total number concentrations in the two chambers. The particle number concentrations remained below 10 cm^{-3} in both chambers for several hours. The aerosol mass concentration (not shown) was less than 0.01 $\mu g\ m^{-3}$. This suggests that clean conditions can be maintained for both chambers for the duration of a typical field experiment.

3.2 Chamber similarity

Similar results should be obtained when identical experiments take place in the two chambers in order to safely use one of them as reference. To establish this, ambient air was introduced in both chambers and the evolution of the concentrations and composition of the particulate matter and gas pollutants was measured. An SMPS measured the size distribution and an AMS the particulate composition. The measured chamber and ambient mass concentrations (Figure 3a) and the AMS spectra (Figures 3c and d) were in good agreement between the two chambers and the ambient. The particle mass concentration in the chambers was approximately 85% of the ambient levels. The theta angle (Kostenidou et al., 2009) between the organic aerosol spectra in the two chambers and the ambient air was in the range of 2.5-6 degrees, suggesting that identical results can be

obtained when filling these chambers with ambient air and that the filling process does not contaminate the air sample.

Pump and tubing losses during the filling procedure were evaluated in order to establish the difference between ambient concentrations and the ones obtained in the chambers. The same number distributions are achieved in both chambers after filling them with ambient air. The penetration efficiency through the tubing and the pump for particles with diameter larger than 80 nm is close to 100%, while for smaller particles due to higher diffusional deposition the penetration efficiency is 45%.

3.3 Particle wall losses

Loss of particles to the walls is one of the processes that complicate the analysis of smog chamber experiments. The use of smaller reactors with lower surface to volume ratios can accelerate these losses. Disturbances of the Teflon reactors tend to increase the wall loss rates due to the buildup of static charges on the chamber walls. Transporting and installing the reactors also results in higher wall loss rate constants (Wang et al., 2018).

In order to assess the wall loss behavior of the system experiments were conducted both in the laboratory and in the field. In all cases, ammonium sulfate seeds were added to the chambers and their decay with time was measured. Typically, the chambers were first filled with clean (particle free) air and then ammonium sulfate seeds were introduced. A solution of 5 g L^{-1} ammonium sulfate was used for the atomizer and a flow rate of 2 L min^{-1}. The decay of the particles was monitored by an SMPS. Size dependent wall loss rate constants were calculated correcting for coagulation (Wang et al., 2018). Figure 4a represents the average size dependent profiles for the loss rate constant K_c of the two chambers for the laboratory experiments. On the field, higher rate loss constants were measured (Figure 4b). For example, loss rate constants of 0.2 h^{-1} were measured for the 350 nm particles in the lab, while for the same size range, a value of approximately 0.5 h^{-1} was measured in the field. Figure 4c and 4d show the wall loss profiles of the two chambers when deployed in the Finokalia campaign over three days of measurements. In both chambers the wall loss rate constants were decreasing over time.

For this reason, the particle wall loss rates are measured after each experiment, by the addition of ammonium sulfate seeds as a final step. The chambers in the laboratory underwent minimum handling during each experiment and thus achieved low loss rate constants for a wide

range of particle sizes. The chambers deployed in the field had higher particle wall-loss rate constants, due to higher static charges on them. The static charge originated from the transportation and handling of the chambers.

In order to assess if it is possible to minimize such charges a test was conducted in the Teflon reactors in the lab. The chambers were moved in a different location inside the building where the lab is located. The two reactors were handled in exactly the same way simulating the handling during a field deployment. One of the chambers was inflated with air to almost half-full while the other was empty. The particle wall-losses were measured before and after the movement. Figure 5 represents the loss rate constants in the two chambers because of the movement. The loss rate did not change in the partially inflated chamber. The other chamber though experienced an increase in the loss rate constants, almost doubling for the particles in the range 50-200 nm, due to stronger friction of the Teflon walls with each other and thus building static charge. No significant change was noticed for particle larger than 250 nm.

3.4 VOC concentrations

Concentrations of the VOCs measured by the PTR-MS were within a few percent of their ambient levels. In most cases, no noticeable differences were seen. Tests indicated that there was no detectable contamination due to the metal bellows pump during the filling process of the two chambers.

4. Laboratory testing

The performance of the system in use tested in experiments that took place indoors at Carnegie Mellon University (Center for Atmospheric Particle Studies – CAPS). The potential aging of urban background air masses in Pittsburgh, PA, by OH radicals was used as a pilot study for the system evaluation. Fewer UV lights were used in this test resulting in a J_{NO2} equal to 0.03 min^{-1}.

4.1 Experimental procedure

Prior to the experiment, both chambers were flushed with particle-free air overnight under UV illumination to remove any residual particles and gas-phase organics. Both chambers were filled with ambient air using the metal bellows pump. During the filling procedure, the instruments were measuring ambient conditions. After the addition of ambient air in the chambers, d9-butanol (60

ppb) was added to both of them as an OH tracer (Barment et al., 2012). The OH levels can be estimated by the decay in the d9-butanol concentration measured be the PTR-MS system at *m*/*z* 66. The reaction constant for the butanol reaction with OH is 3.4 x 10^{12} cm^3 $molecules^{-1}$ s^{-1}. HONO was injected only into the perturbation chamber for about 3 min to produce OH upon UV illumination. The UV lights then turned on were illuminating both chambers. After the completion of the perturbation experiment, a seed wall-loss experiment was conducted to quantify the particle wall-loss rate constants for the two chambers as described in section 3.3.

4.2 Results and discussion

The wall-loss corrected total particle number concentration as measured by the SMPS are shown in Figure 6. The instruments were measuring ambient conditions during the filling process. The average ambient number concentration was around 2500 cm^{-3}. HONO was injected in the perturbed chamber at t=0.4 h. After turning on the UV lights (t=0.6 h) an increase in the total particle number and volume in the perturbed chamber was observed while no change in the control chamber was noticed. The increase in the perturbed chamber is due to the formation of new particles (Figure 7).

Based on the AMS measurements, the ambient air used to fill the chambers contained on average 3.6 μg m^{-3} of non-refractory PM_1 with organics accounting for 75%, sulfate 17%, ammonium 6% and nitrate 2%. The collection efficiency of the AMS measurements was found to be 0.6 based on the algorithm of Kostenidou et al. (2007), while the estimated OA density was 1.2 g cm^{-3}. The calculated theta angle (Kostenidou et al., 2009) between the ambient and the chamber organic mass spectra vectors was around 5 degrees, indicating that the aerosol composition inside the chamber was essentially the same as in the ambient.

To quantify the secondary aerosol formation, data were corrected for both the collection efficiency and for particle wall-losses. Figure 8 shows the concentrations of the major PM_1 components in the two chambers. An increase of concentration was observed in the perturbed chamber. After 2.5 hours of exposure to OH an additional 1.5 μg m^{-3} of organics, 0.2 μg m^{-3} of sulfates, 0.1 μg m^{-3} of nitrates and 0.1 μg m^{-3} of ammonium was formed. The average OH concentration in the perturbed chambers was 8.0×10^6 molecules cm^{-3} corresponding to approximately 11 h of equivalent exposure to an ambient OH=1.5×10^6 molecules cm^{-3}. The OH concentration in the control chamber was an order of magnitude less 8×10^5 molecules cm^{-3}. The

organic spectra of the additional formed SOA and the initial OA in the perturbed chamber were relatively similar; their theta angle was 10 degrees (Figure 9). The mass spectrum of the processed OA characterized by lower fractional contributions at *m*/*z* 43 and 44.

The evolution of the oxygen to carbon ratio of the organic aerosol in the two chambers is shown in Figure 10. The O:C of the ambient organic aerosol and of the initial OA in the two chambers was 0.44. After the OH introduction and the SOA production in the perturbed chamber, the O:C decreased slightly to 0.40. The O:C in the control chamber remained approximately the same. The decrease of the O:C in the perturbed chamber indicates that the additional formed SOA had smaller O:C than the ambient.

5. Conclusions

A portable dual chamber system has been developed for field studies using ambient air as a starting point. The system has been evaluated and no contamination was observed during a typical experiment. The concentration in the two chambers when filled with ambient air are within a few percent of each other. Particle losses during filling were less than 20%. No noticeable losses or cross-contamination was observed for the measured VOC species.

Higher wall loss rates were observed when the chambers were deployed in the field, compared to the lower and stable rates observed when the chambers were inside the laboratory, due to higher electrostatic charges induced during their movement. A reduction in the wall loss rates was observed when the chambers are deployed in the field, suggesting that they should be measured after each experiment. The losses can be reduced if the chambers are transported partially inflated. Initial laboratory experiments show promising results in respect to potential aging properties of urban background air in Pittsburgh. An additional 1.5 μg m^{-3} of SOA was formed after 12 h of equivalent OH exposure with a moderate decrease of the O:C ratio. Implementing the system in the field will enable the study of complex systems that were previously out of reach with traditional stationary chamber facilities.

Data availability. The data in the study are available from the authors upon request (spyros@chemeng.upatras.gr).

Author contributions. CK constructed the facility, participated in the experiments and wrote the paper. SJ conducted, analysed the wall loss and test experiments and contributed to the writing of the paper. EL and KF helped in the construction of the facility and assisted in the experiments. SNP was responsible for the design of the study, the synthesis of the results and contributed to the writing of the paper.

Competing interests. The authors declare that they have no conflict of interest.

Acknowledgements. This research was supported by the European Research Council Project ATMOPACS (Atmospheric Organic Particulate Matter, Air Quality and Climate Change Studies) (Grant Agreement 267099). This work has also received funding from the European Union's Horizon 2020 research and innovation programme through the EUROCHAMP-2020 Infrastructure Activity under grant agreement No 730997.

References

Barmet, P., Dommern, J., DeCarlo, P. F., Tritscher, T., Praplan, A. P., Platt, S. M., and Prevot, A. S. H.: OH clock determination by proton transfer reaction mass spectrometry at an environmental chamber. Atmos. Meas. Tech., 5, 647–656, 2012.

Carter, W. P. L., Cocker, D. R., Fitz, D. R., Malkina, I. L., Bumiller, K., Sauer, C. G., Pisano, J. T., Bufalino, C., and Song, C.: A new environmental chamber for evaluation of gas-phase chemical mechanisms and secondary aerosol formation, Atmos. Environ., 39, 7768–7788, 2005.

Cocker D. R., Clegg, S. L., Flagan, R. C., and Seinfeld, J. H.: The effect of water on gas–particle partitioning of secondary organic aerosol. Part I: a-pinene/ozone system. Atmos. Environ., 35, 6049–6072, 2001b.

Cocker, D. R., Flagan, R. C., and Seinfeld, J. H.: State-of-the-art chamber facility for studying atmospheric aerosol chemistry, Environ. Sci. Technol., 35, 2594-2601, 2001a.

Finlayson, B., Pitts, J. N.: Photochemistry of the polluted troposphere. Science, 192, 111-119, 1976.

Hallquist, M., Wenger, J. C., Baltensperger, U., Rudich, Y., Simpson, D., Claeys, M., Dommen, J., Donahue, N. M., George, C., Goldstein, A. H., Hamilton, J. F., Herrmann, H.,

341 Hoffmann, T., Iinuma, Y., Jang, M., Jenkin, M. E., Jimenez, J. L., Kiendler-Scharr, A.,
342 Maenhaut, W., McFiggans, G., Mentel, T. F., Monod, A., Prevot, A. S. H., Seinfeld, J. H.,
343 Surratt, J. D., Szmigielski, R. and Wildt, J.: The formation, properties and impact of
344 secondary organic aerosol: current and emerging issues. Atmos. Chem. Phys., 9, 5155–
345 5236, 2009.
346 Heisler, S. L., and Friedlander, S. K.: Gas to particle conversion in photochemical smog: Aerosol
347 growth laws and mechanisms for organics, Atmos. Environ., 11, 157-168, 1977.
348 Hennigan, C. J., Miracolo, M. A., Engelhart, G. J., May, A. A., Presto, A. A., Lee, T., Sullivan, A.
349 P., McMeeking, G. R., Coe, H., Wold, C.E., Hao, W. M., Gilman, J. B., Kuster, W. C.,
350 deGouw, J., Schichtel, B. A., Collett Jr., J. L., Kreidenweis, S. M., and Robinson, A. L. \:
351 Chemical and physical transformations of organic aerosol from the photo-oxidation of open
352 biomass burning emissions in an environmental chamber, Atmos. Chem. Phys., 11, 7669–
353 7686, 2011.
354 Hoffmann, T., Odum, J. R., Bowman, F., Collins, D., Klockow, D., Flagan, R. C., and Seinfeld, J.
355 H.: Formation of organic aerosols from the oxidation of biogenic hydrocarbons. J. Atmos.
356 Chem. 26, 189–222, 1997.
357 Jeffries, H., Fox, D., and Kamens, R.: Outdoor smog chamber studies: light effects relative to
358 indoor chambers, Environ. Sci. Technol., 10, 1006-1011, 1976.
359 Kaltsonoudis, C., Kostenidou, E., Louvaris, E., Psichoudaki, M., Tsiligiannis, E., Florou, K.,
360 Liangou A., and Pandis, S. N.: Characterization of fresh and aged organic aerosol
361 emissions from meat charbroiling, Atmos. Chem. Phys. 17, 7143–7155, 2017.
362 Kelly, N. A., and Gunst, R. F.: Response of ozone to changes in hydrocarbon and nitrogen oxide
363 concentrations in outdoor smog chambers filled with Los Angeles air, Atmos. Environ.,
364 24, 2991-3005, 1990.
365 Kelly, N. A.: The photochemical formation and fate of nitric acid in the metropolitan Detroit area:
366 Ambient, captive-air irradiation and modeling results, Atmos. Environ., 21, 2163-2177,
367 1987.
368 Kim, Y. J., Platt, U., Gu, M. B., and Iwahashi, H.: Atmospheric and biological environmental
369 monitoring, Springer, 2009.

370 Kostenidou, E., Pathak, R. K., and Pandis, S. N.: An algorithm for the calculation of secondary
371 organic aerosol density combining AMS and SMPS data, Aerosol Sci. Technol., 41, 1002–
372 1010, 2007.
373 Kostenidou, E., Lee, B. H., Engelhart, G. J., Pierce, J. R., and Pandis, S. N.: Mass spectra
374 deconvolution of low, medium and high volatility biogenic secondary organic aerosol,
375 Environ. Sci. Technol., 43, 4884–4889, 2009.
376 Kostenidou, E., Kaltsonoudis, C., Tsiflikiotou, M., Louvaris, E., Russell, L. M. and Pandis, S. N.:
377 Burning of olive tree branches: a major organic aerosol source in the Mediterranean.
378 Atmos. Chem. Phys., 13, 8797–8811, 2013.
379 Kouvarakis, G., Tsigaridis, K., Kanakidou, M., and Mihalopoulos, N.: Temporal variations of
380 surface background ozone over Crete island in the southeast Mediterranean, J. Geophys.
381 Res., 105, 4399-4407, 2000.
382 Laity, J.: A smog chamber study comparing blacklight fluorescent lamps with natural sunlight,
383 Environ Sci. Technol., 5, 1218-1220, 1971.
384 Lee, B. S., Bae, G. N., Moon, K. C., Choi, M.: Correlation between light Intensity and ozone
385 formation for photochemical smog in urban air of Seoul, Aerosol Air Qual. Res., 10, 540-
386 549, 2010.
387 Leone, J. A, Flagan, R.C., Grosjean, D. and Seinfeld, J.H.: An outdoor smog chamber and
388 modeling study of toluene–NO_x photooxidation. Int. J. Chem. Kinetics, 17, 177–216, 1985.
389 Pathak, R. K., Stanier, C. O., Donahue, N. M., and Pandis, S. N.: Ozonolysis of alpha-pinene at
390 atmospherically relevant concentrations: Temperature dependence of aerosol mass
391 fractions (yields), J. Geophys. Res, 112, D03201, doi: 10.1029/2006jd007436, 2007.
392 Paulsen, D., Dommen, J., Kalberer, M., Prevot, A. S. H., Richter R., Sax, M., Steinbacher, M.,
393 Weingartner, E., and Baltensperger, U.: Secondary organic aerosol formation by irradiation
394 of 1,3,5-trimethylbenzene - NO_x-H_2O in a new reaction chamber for atmospheric chemistry
395 and physics, Environ. Sci. Technol., 39, 2668-2678, 2005.
396 Pitts, J. N., Smith, J. P., Fitz, D. R., and Grosjean, D.: Enhancement of photochemical smog by
397 N,N diethylhydroxylamine in polluted ambient air, Science, 197, 255–257, 1977.
398 Platt, S. M., El-Haddad, I., Zardini, A. A., Clairotte, M., Astorga, C., Wolf, R., Slowik, J. G.,
399 Temime-Roussel, B., Marchand, N., Ježek, I., Drinovec, L., Močnik, G., Möhler, O.,
400 Richter, R., Barmet, P., Bianchi, F., Baltensperger, U., and Prévôt, A. S. H.: Secondary

organic aerosol formation from gasoline vehicle emissions in a new mobile environmental reaction chamber. Atmos. Chem. Phys., 13, 9141-9158, 2013.

Roberts, P. T, and Friedlander, S. K.: Photochemical aerosol formation. SO_2, 1-heptene, and NO, in ambient air, Environ. Sci. Technol., 10, 573-580, 1976.

Shibuya, K., and Nagashima, T.: Photochemical ozone formation in the irradiation of ambient air samples by using a mobile smog chamber, Environ. Sci. Technol., 6, 661-665, 1981.

Stockwell, C. E., Yokelson, R. J., Kreidenweis, S. M., Robinson, A. L., DeMott, P. J., Sullivan, R. C., Reardon, J., Ryan, K. C., Griffith, D. W. T., and Stevens, L.: Trace gas emissions from combustion of peat, crop residue, domestic biofuels, grasses, and other fuels: configuration and Fourier transform infrared (FTIR) component of the fourth fire lab at Missoula experiment (FLAME-4), Atmos. Chem. Phys., 14, 9727–9754, 2014.

Tritscher, T., Dommen, J., DeCarlo, P. F., Gysel, M., Barmet, P. B., Praplan, A. P., Weingartner, E., Prévôt, A. S. H., Riipinen, I., Donahue, N. M., and Baltensperger, U.: Volatility and hygroscopicity of aging secondary organic aerosol in a smog chamber. Atmos. Chem. Phys., 11, 11477-11496, 2011.

Tkacik, D. S., Lambe, A. T., Jathar, S., Li, X., Presto, A. A., Zhao, Y., Blake, D. R., Meinardi, S., Jayne, J. T., Croteau, P. L., and Robinson, A. L.: Secondary organic aerosol formation from in-use motor vehicle emissions using a potential aerosol mass reactor. Environ. Sci. Technol., 48, 11235–11242, 2014.

Ortega, A. M., Hayes, P. L., Peng, Z., Palm, B. B., Hu, W. W., Day, D. A., Li, R., Cubison, M. J., Brune, W. H., Graus, M., Warneke, C., and Gilman, J. B.: Real-time measurements of secondary organic aerosol formation and aging from ambient air in an oxidation flow reactor in the Los Angeles area. Atmos. Chem. Phys., 16, 7411–7433, 2016.

Wang, N., Jorga, S. D., Pierce, J. R., Donahue, N. M., and Pandis, S. N.: Particle wall-loss correction methods in smog chamber experiments, Atmos. Meas. Tech. Discuss., doi:10.5194/amt-2018-175, 2018.

Warren, B., Song, C., and Cocker, D.R.: Light intensity and light source influence on secondary organic aerosol formation for the m-xylene/NOx photooxidation system, Environ. Sci. Technol., 42, 5461–5466, 2008.

Weitkamp, E. A., Sage, A. M., Pierce, J. R., Donahue, N. M., and Robinson, A.L.: Organic aerosol formation from photochemical oxidation of diesel exhaust in a smog chamber. Environ. Sci. Technol., 410, 6969–6975,

Atmos. Meas. Tech. Discuss., https://doi.org/10.5194/amt-2018-394
Manuscript under review for journal Atmos. Meas. Tech.
Discussion started: 4 December 2018

Figure 1. Pictures of the portable dual chamber system: a) the dual chambers; b) UV light assembly; c) field deployment during the FAME 16 study; d) system configuration with the UV lights on and the top cover open.

Atmos. Meas. Tech. Discuss., https://doi.org/10.5194/amt-2018-394
Manuscript under review for journal Atmos. Meas. Tech.
Discussion started: 4 December 2018

Atmospheric Measurement Techniques Discussions

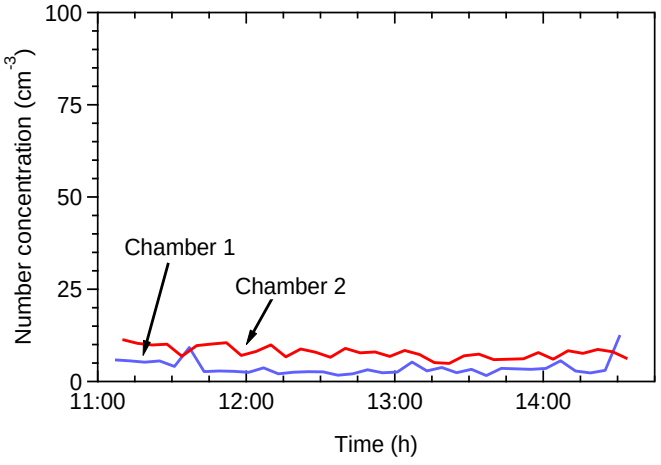

Figure 2. Total particle number concentrations as a function of time when the chambers were filled with clear air in the field for leak check of the chambers.

Atmos. Meas. Tech. Discuss., https://doi.org/10.5194/amt-2018-394
Manuscript under review for journal Atmos. Meas. Tech.
Discussion started: 4 December 2018

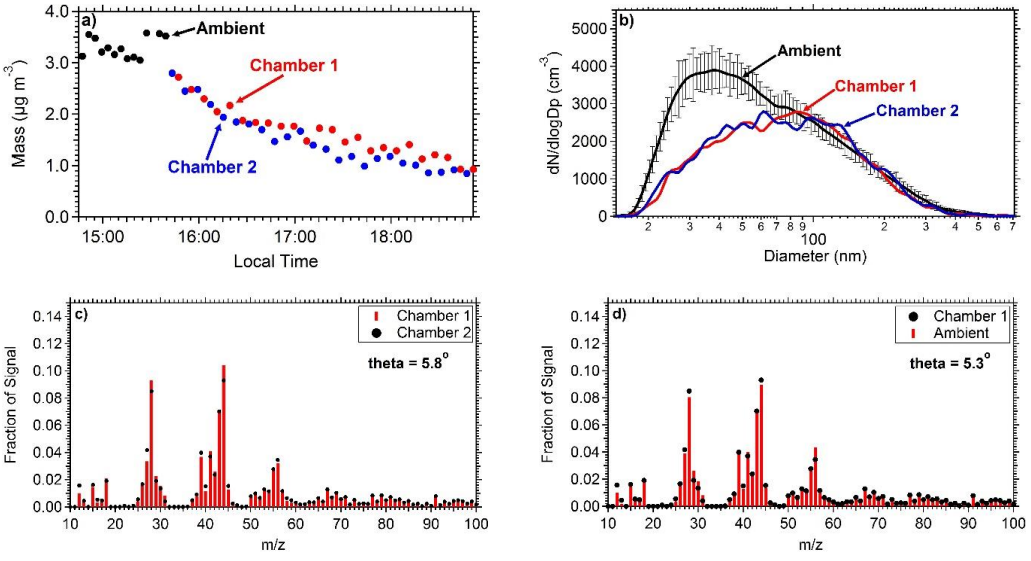

Figure 3. Comparison of the measurements between the two chambers and between ambient measurements: a) Mass concentration ($PM_{0.7}$) as measured by the SMPS in both the chambers and the ambient. b) Number distributions inside the chambers and in the ambient (the error bar represent one standard deviation). c) Average aerosol mass spectra of chamber 1 and chamber 2 filled with ambient air. d) Average aerosol mass spectra of ambient air and chamber 1.

Atmos. Meas. Tech. Discuss., https://doi.org/10.5194/amt-2018-394
Manuscript under review for journal Atmos. Meas. Tech.
Discussion started: 4 December 2018

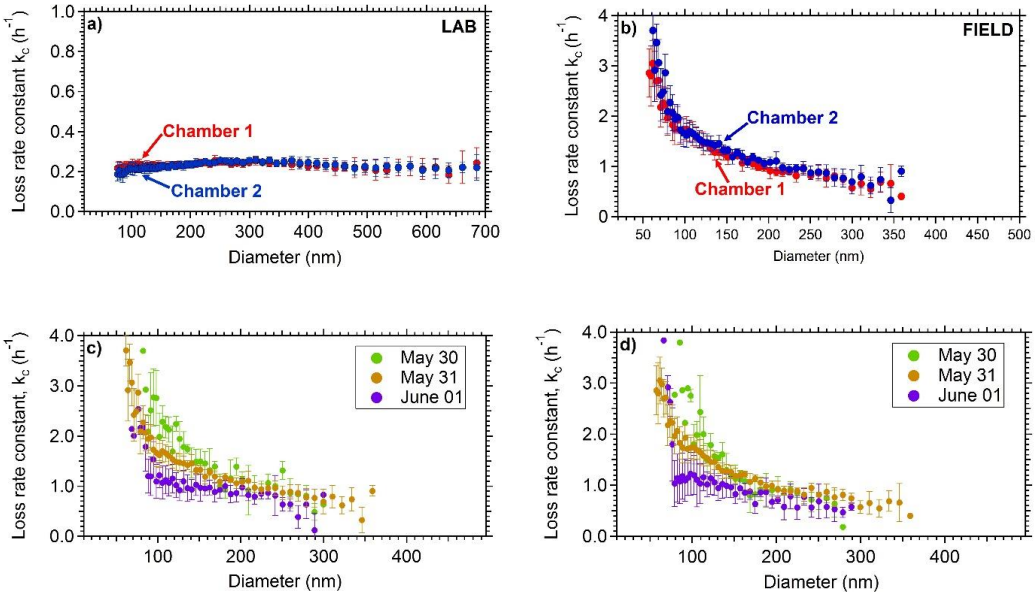

Figure 4. Coagulation-corrected particle wall-loss rate constant as a function of particle size for the two chamber a) in the laboratory and b) in the field. The particle wall-loss rate constant as a function of particle size during three consecutive days for the field deployment. Figure c corresponds to chamber 1 and d) to chamber 2.

Atmos. Meas. Tech. Discuss., https://doi.org/10.5194/amt-2018-394
Manuscript under review for journal Atmos. Meas. Tech.
Discussion started: 4 December 2018

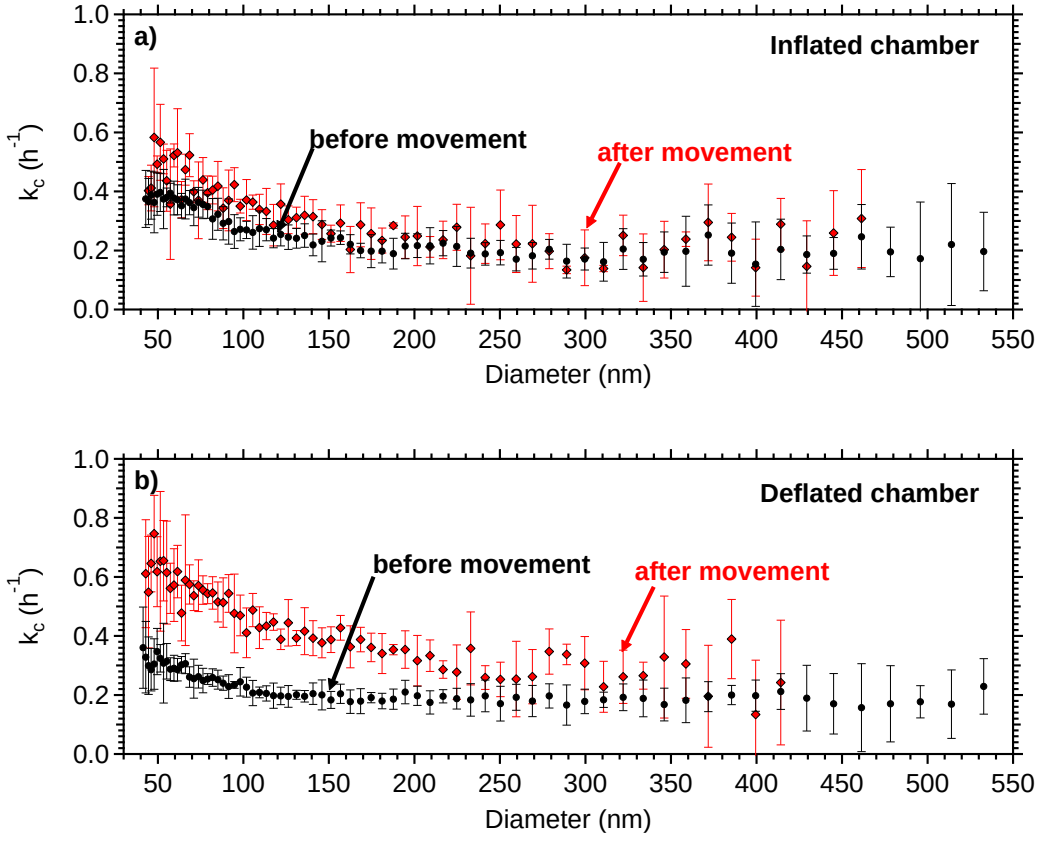

Figure 5. Coagulation-corrected particle wall-loss rate constant as a function of particle size for the two chamber after the movement a) in the partially inflated chamber and b) in the deflated chamber. The error bars represent one standard deviation.

Atmos. Meas. Tech. Discuss., https://doi.org/10.5194/amt-2018-394
Manuscript under review for journal Atmos. Meas. Tech.
Discussion started: 4 December 2018

Atmospheric Measurement Techniques Discussions

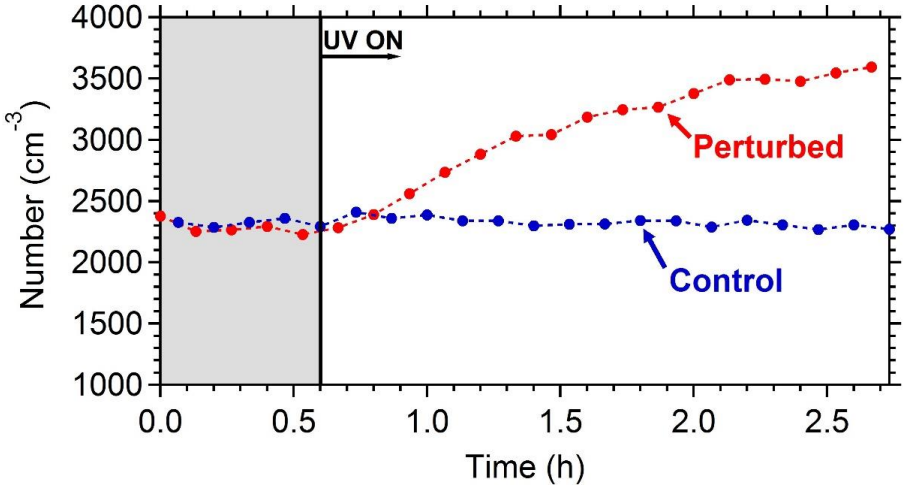

510

511 **Figure 6.** The wall-loss corrected SMPS-measured aerosol number concentration. HONO was
512 added only in the perturbed chamber at *t*= 0.4 h to produce OH under UV illumination. The shaded
513 area indicates that the chambers were dark.

514

515

516

517

518

519

520

521

522

523

Atmos. Meas. Tech. Discuss., https://doi.org/10.5194/amt-2018-394
Manuscript under review for journal Atmos. Meas. Tech.
Discussion started: 4 December 2018

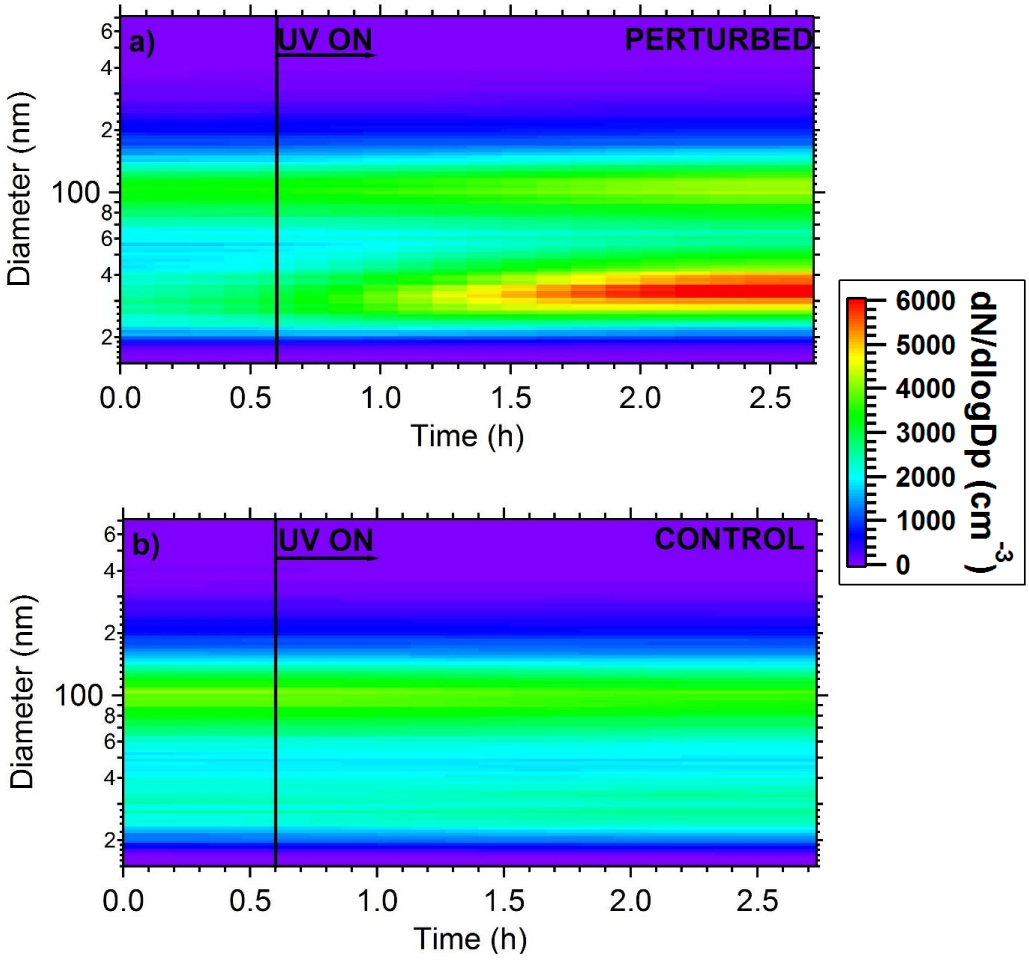

524 **Figure 7.** Plots of the evolution of particle number distributions during the HONO perturbation
525 experiment in Pittsburgh. (a) Perturbed chamber and (b) Control chamber.

Atmos. Meas. Tech. Discuss., https://doi.org/10.5194/amt-2018-394
Manuscript under review for journal Atmos. Meas. Tech.
Discussion started: 4 December 2018

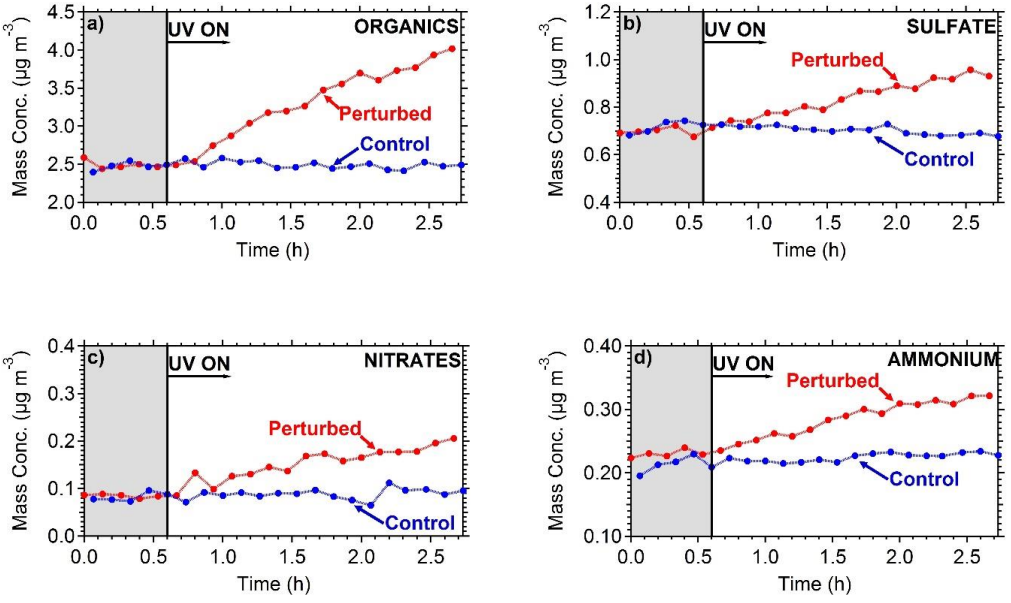

Figure 8. The particle wall-loss corrected concentrations of the major PM_1 components measured by the AMS a) organics, b) sulfate, c) nitrates and d) ammonium. The shaded area indicates that the chambers were dark. Data have been corrected for the collection efficiency (CE=0.6).

Atmos. Meas. Tech. Discuss., https://doi.org/10.5194/amt-2018-394
Manuscript under review for journal Atmos. Meas. Tech.
Discussion started: 4 December 2018

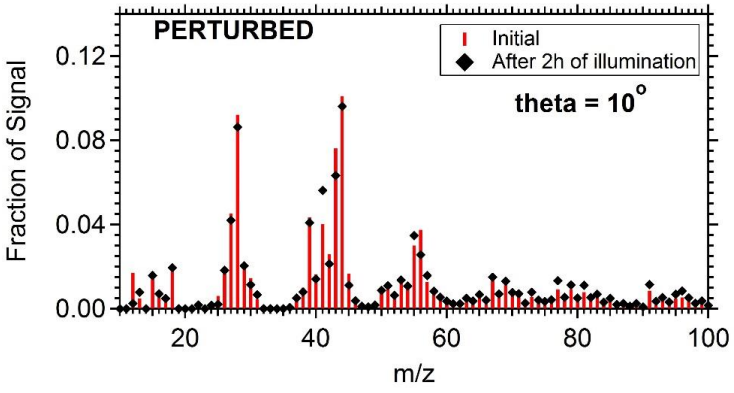

544 **Figure 9.** The organic mass spectra after filling and after two hours of UV illumination in the
545 perturbed chamber.
546
547
548
549
550
551
552
553
554
555
556
557
558
559
560

Atmos. Meas. Tech. Discuss., https://doi.org/10.5194/amt-2018-394
Manuscript under review for journal Atmos. Meas. Tech.
Discussion started: 4 December 2018

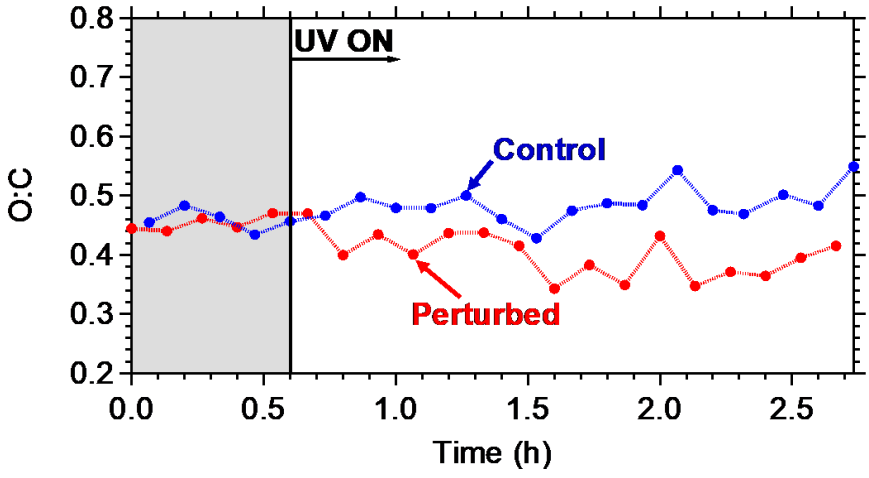

Figure 10. The O:C ratio evolution for the control and the perturbed chamber. The shaded area indicates that the chambers were in the dark.